Korean J. Chem. Eng., 39(1), 178-188 (2022)
DOI: 10.1007/s11814-021-0935-9

pISSN: 0256-1115
eISSN: 1975-7220

Investigation of thin-film composite hollow fiber forward osmosis membrane for osmotic concentration: A pilot-scale study

Rem Jalab*, Abdelrahman Mohammed Awad*, Mustafa Saleh Nasser*,†, Ibnelwaleed Ali Hussein*, Fares Almomani, Joel Minier-Matar***, and Samer Adham*****

*Gas Processing Centre, College of Engineering, Qatar University, Doha, Qatar
**Department of Chemical Engineering, College of Engineering, Qatar University, Doha, Qatar
***ConocoPhillips Global Water Sustainability Centre, Qatar Science & Technology Park, Doha, Qatar
(*Received 3 February 2021 • Revised 6 July 2021 • Accepted 21 August 2021*)

Abstract–The current study applied the forward osmosis (FO) based osmotic concentration (OC) process at the pilot-scale for concentrating synthetic feed solution (FS). The process water (PW) salinity represents effluents from the gas industry, while the draw solution (DS) mimics seawater. Besides, the performance of a hollow fiber (HF) membrane manufactured from polyamide thin film composite (PA-TFC) was evaluated. The effect of operation with various feed recovery rates, flowrates and temperatures on the OC performance was examined. Outcomes reveal that the tested membrane succeeded in recovering up to 90% of FS at water flux of 6.40 LMH. The stability of OC plant was successfully demonstrated for 48 hours long-term run at 75% feed recovery as an optimum condition, where the TFC membrane achieved average water flux of 6.00 LMH, respectively. Higher DS flowrate improved the OC performance by inducing higher water permeation and FS recovery; however, it increased the undesirable reverse solute diffusion. Lastly, the permeability coefficient of the HF membrane was estimated by 2.69 LMH/bar at 25 °C, which significantly enhanced at higher temperatures.

Keywords: Pilot-scale, Osmotic Concentration (OC), Hollow Fiber (HF), Membrane, Polyamide Thin-film Composite (PA-TFC)

INTRODUCTION

Osmosis is the physical phenomenon represented by the natural transport of the water through a membrane of selective permeability from the low concentration solution side to the side of higher solution's concentration. The passage of water across the permeability selective membrane is a result of the osmotic pressure difference ($\Delta\pi$) caused by salt concentration gradient. Generally, there are three different types for the osmosis based membrane processes: forward osmosis (FO), reverse osmosis (RO) and pressure retarded osmosis (PRO) (Fig. 1). FO technology exploits the naturally occurring osmosis, whereas RO requires applying hydraulic pressure greater than the osmotic pressure ($P>\Delta\Pi$) to the high concentration side to transfer water to the diluted side. Alternatively, to transfer water to the concentrated side in PRO, a hydraulic pressure lower than $\Delta\Pi$ is to be applied to the same high concentration side.

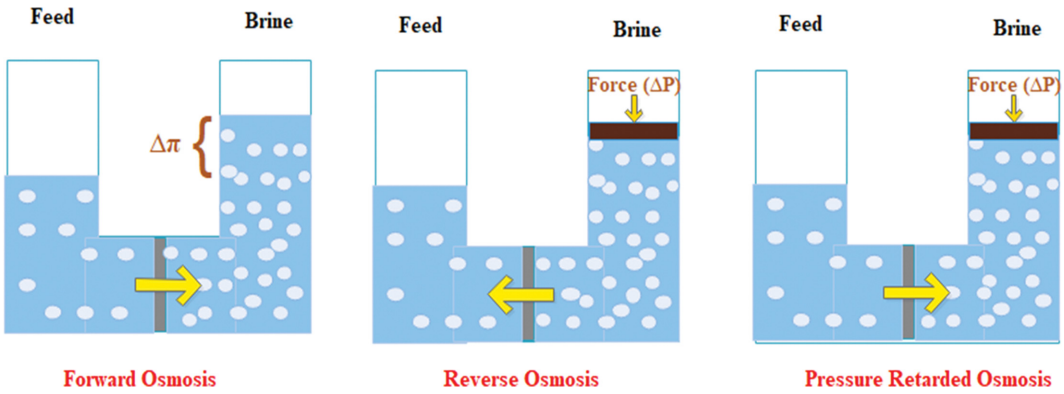

Fig. 1. Osmosis based membrane processes.

†To whom correspondence should be addressed.
E-mail: m.nasser@qu.edu.qa

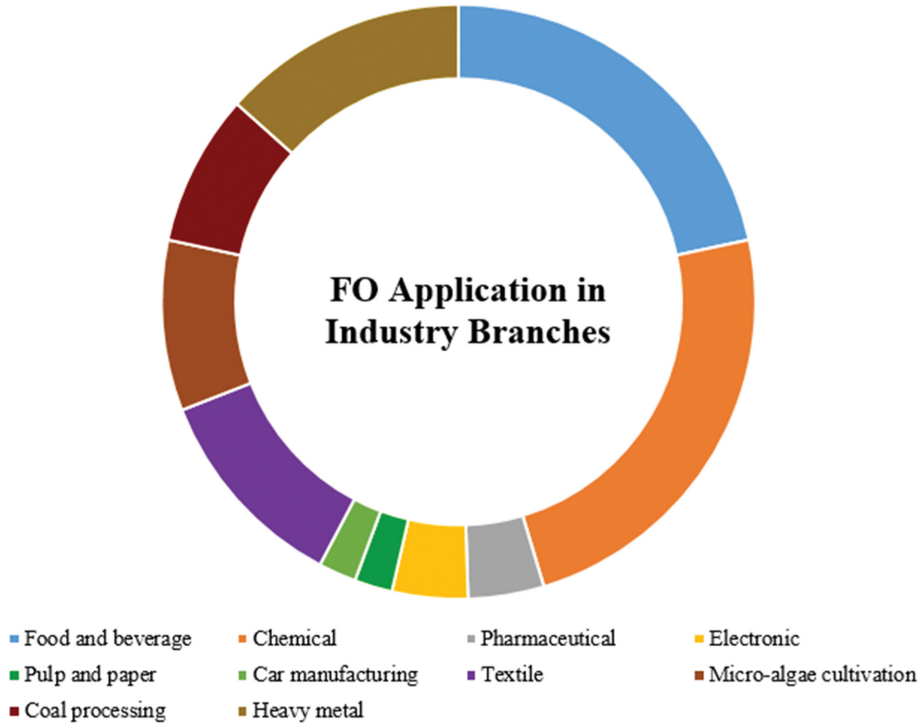

Fig. 2. Industrial applications of FO technology.

FO technology has gained renewed research interests for its versatile potential in areas of wastewater treatment and water reuse [1,2]. The FO process harnesses the osmotic pressure difference between diluted feed solution (FS) and concentrated draw solution (DS) across semipermeable membrane to induce water permeation [3-6]. With the continued water permeation, the FS becomes concentrated and DS salinity is reduced, resulting in diminished separation driving force that requires the recovery of DS salinity. Thereupon, FO is usually operated in two steps encompassing the membrane separation with additional DS recovery step. Several advantageous features of FO have made it a distinctive technology, raising research interest in recent years. The paramount features of FO comprise high solute rejection [3], irreversible fouling [7], high fouling resistance [8], proved reliability and tolerance of high salinity feed streams [9]. When compared with the RO process, the exclusion of hydraulic pressure application guarantees considerably lower energy consumption for the FO [10,11]. It was reported that desalination with FO-low pressure RO hybrid process recorded 1.5 kWh/m^3 energy consumption compared to 2.5 kWh/m^3 consumed by seawater RO (SWRO) process [12]. Due to the feasible adaption in the reclamation of complex and high strength feed streams, FO appears to be a promising process for a diverse set of industries [13] (Fig. 2).

In spite of the aforementioned attributes, the operation of FO is challenged by concentration polarization and reverse solute diffusion [14]. These phenomena occur due to the difference in concentration between FS and DS across the membrane layers, resulting in diminished osmotic gradient and water permeation [15]. Although FO fouling has minimal detrimental effect on performance of the process due to less acute cake layer formed on membrane surface if compared with RO [16], the fouling in FO remains a challenge that reduces the water permeability and plugs the membrane pores [17].

Nonetheless, DS is usually recovered using energy intensive nanofiltration (NF), RO or membrane distillation (MD) [18,19], rendering the implementation of FO an economic challenge [14]. However, operated as an osmotic concentration (OC) process with eliminated DS recovery step, FO is considered a cost-effective membrane-based treatment technology [5,20,21]. Fertilizer drawn forward osmosis (FDFO) is an example to FO process operating without DS recovery for the use of diluted DS in irrigation. It is reported that FDFO has 23% lower total water cost of 0.66 \$/m^3 than RO system (0.86 \$/m^3) used for the irrigation purpose [22]. Additionally, FO benefit of producing diluted DS is exploited for operating FO as pretreatment before RO, hence reducing the energy requirement of the downstream RO. Recently, an economic study revealed 20% lower net present value (NPV) for the desalination of high saline water using membrane bioreactor (MBR)-FO-RO compared to MBR-RO process Make it [23]. In OC process, the single filtration step in FO technology is applied alone providing concentrated FS at reduced volume as in Fig. 3.

Produced and process water from oil and gas exploration is managed through deep well injection for disposal or use for enhanced recovery after being invalid for minimization and recycling purposes [24,25]. About 80% of produced water is injected back to the same formation for pressure maintenance [19]. However, the toxic nature of the produced water containing toxic compounds and resulting in undesirable environmental consequences promoted the need for water treatment. In fact, FO as an OC process is best suited for volume reduction of wastewater injected into underground wells

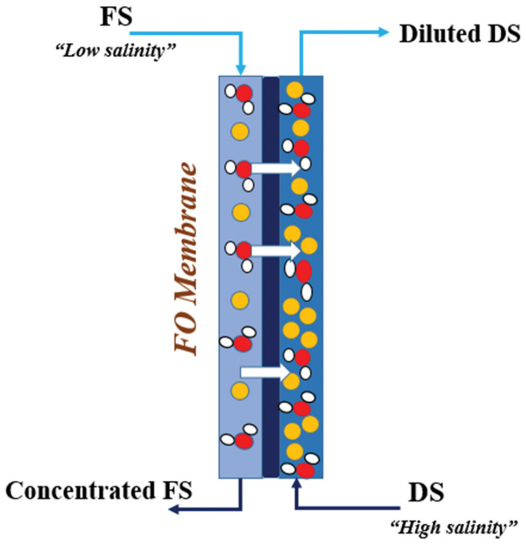

Fig. 3. FO-based OC process scheme.

after being produced from oil and gas well drilling activities [2]. The FO process possesses superior attributes pertaining to high achievable water recovery with low energy consumption and high fouling resistance [3,8]. These attributes have boosted the implementation of FO-based processes for high-strength water treatment and concentration [9]. In two bench-scale investigations employed for OC, FO successfully fulfilled 50% and 80% volume reduction of drilling and produced wastewater, respectively [26-28]. Despite the promising outcome of OC implementation, the process has not been investigated at larger scale with typical operating conditions relevant to industry such as feed water characteristics, flowrates, recovery rate, and operation time.

Despite the good potential of FO-based processes, efforts must be devoted to tackling some existing challenges encompassing concentration polarization, reverse solute flux and fouling [14]. These operational challenges crucially deteriorate the process performance by obstructing the water permeation. Reverse solute diffusion and concentration polarization (CP) phenomena resulting in the decline of osmotic pressure gradient are frequently encountered because of DS solutes back diffusion to FS side, and concentration difference between FS and DS [3,15]. Note that some operating parameters, including feed and draw solutions properties and types, osmotic gradient, inlet cross flowrate and temperature, have a substantial impact on FO-based processes performance [29-33]. The influence of such conditions could be reflected in feed recovery rate, water flux ($L \cdot m^{-2} \cdot h^{-1}$ (LMH)) and reverse solute flux ($mmol \cdot m^{-2} \cdot h^{-1}$) as main performance indicators [34,35].

To ensure widespread application of effective FO-based processes, novel advancements in the FO membranes fabrication by tuning the membrane configuration, support, and active layers' properties are truly required. FO technology improvements continue with performance investigation of flat sheets, spiral wound, plate, and frame modules produced by several commercial companies [36-39]. These FO membranes are ordinarily manufactured from cellulose triacetate (CTA) or the polyamide (PA) and polyelectrolyte based thin film composite (TFC) [40-42]. Lately, Toyobo, Aquaporin and Cheil Industries have developed a new hollow fiber (HF) FO membrane which demonstrated good performance in terms of high permeation flux and low fouling owing to the high packing density and large active area of this configuration [43-47]. The potential of Toyobo HF membrane for wastewater volume reduction was demonstrated in our previous research study [48], where the membrane was capable of achieving maximum of 90% feed recovery. Subsequently, these advantageous attributes of HF membrane allowed its worldwide development in the laboratories of academic institutions such as the TFC-HF membrane fabricated by Singapore Membrane Technology Center, currently being supplied by Aromatec company [27].

In this study, an OC pilot-plant was constructed to evaluate the performance of polyamide based TFC HF membrane for feed concentration and recovery at the pilot-scale level. Through this paper, the effect of achieving different feed recovery rates and role of changing flowrates on the OC performance quantified as water flux, reverse solute flux (RSF) and specific reverse solute flux are demonstrated. Above all, the long-term stability of OC pilot plant was assessed through 48 hours of continuous operation. Lastly, the temperature influence on the intrinsic properties of membranes, represented by water and salt permeability coefficients, is also demonstrated.

MATERIALS AND METHODS

1. Materials

1-1. Feed and Draw Solution

The FS synthetically mimics the Qatari real process water (PW) after membrane bioreactor (MBR) pretreatment. While the DS is a synthetic saline solution comparable to the local seawater salinity. FS was prepared of 2,000 $mg \cdot L^{-1}$ salinity by dissolving industrial-grade NaCl salt (Concord Overseas, India) of 99.62% purity

Table 1. Feed and draw solutions characteristics

Parameter	Feed solution	Draw solution
TDS ($mg \cdot L^{-1}$)	2,000	40,000
TSS ($mg \cdot L^{-1}$)	1.30	15.20
Inorganic carbon (IC) ($mg \cdot L^{-1}$)	18.75	15.40
Total organic carbon (TOC) ($mg \cdot L^{-1}$)	0.32	0.71
pH	7.90	7.74
Conductivity (mS/cm)	4.00	64.00
Turbidity (NTU)	0.15	0.72

in filtered tap water (ATLAS FILTRI, Switzerland). The residual chlorine in filtered tap water was 0.04 $mg \cdot L^{-1}$ measured using the chlorine kit (HACH, US). DS was prepared of 40,000 $mg \cdot L^{-1}$ salinity by mixing the same NaCl salt with the tap water filtered similarly as in FS preparation. The characteristics of FS and DS streams are displayed in Table 1.

1-2. FO Membrane

The utilized thin film HF membrane was supplied by the Singaporean company Aromatec after its development in Singapore Membrane Technology Center (SMTC) under the Nanyang Technological University (NTU) (Fig. 4). The membrane module is of 0.5 m^2 surface area with 1.00 mm outer diameter and 0.67 mm inner diameter. The membrane is fabricated from polyethersulfone substrate with polyamide selective layer. The active layer is at the lumen of HF where the FS is introduced, and the DS is pumped towards the shell side. For outstanding performance, it is recommended to operate the membrane at a flowrate of 1.5 $L \cdot min^{-1}$ for FS and DS. The tolerated operating conditions are residual chlorine ≤1 $mg \cdot L^{-1}$, temperature range from 5-50 °C and pressure of 3 bar and 1 bar for FS and DS sides, respectively.

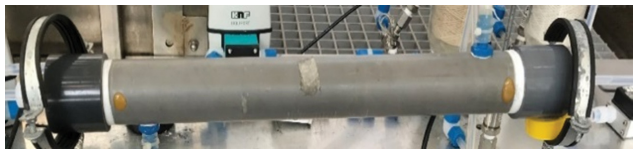

Fig. 4. TFC-HF membrane by Aromatec.

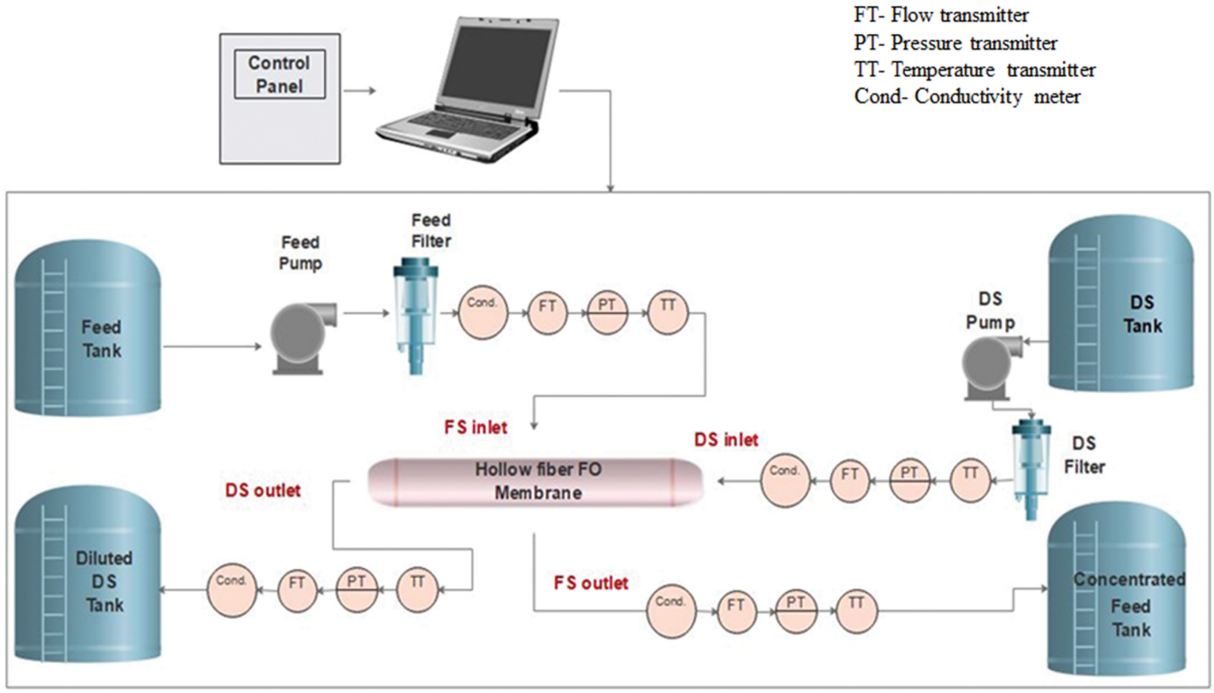

Fig. 5. Schematic diagram of constructed osmotic concentration pilot plant.

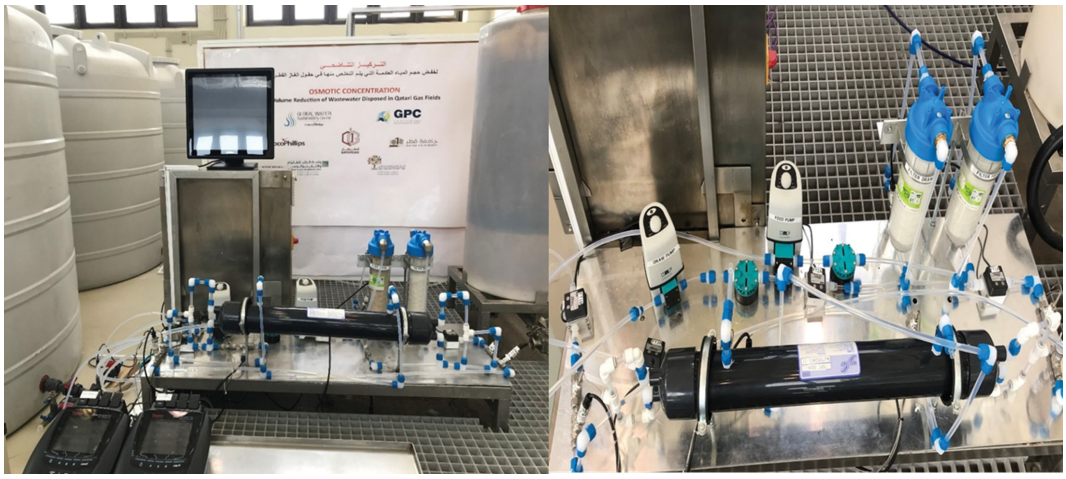

Fig. 6. Real constructed osmotic concentration pilot plant.

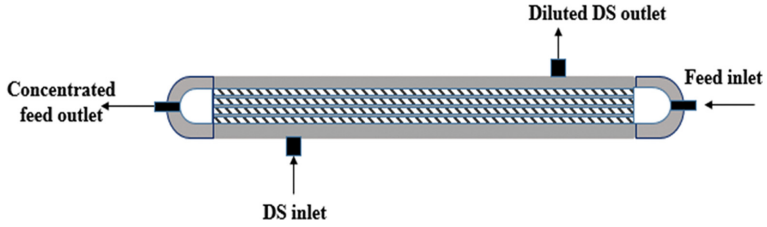

Fig. 7. Inside-out configuration of TFC-HF membrane.

2. Osmotic Concentration (OC) Pilot-plant

A pilot plant of 5,000 L capacity was successfully constructed for the osmotic concentration of the synthetically prepared FS and for reducing its volume. The pilot-plant consists of four tanks for storing FS, DS, concentrated FS and diluted DS as in Fig. 5 and Fig. 6. The cross flow velocity inside the membrane module is created by the two variable speed diaphragm pumps (Model KNF Liquiport, Sterlitech, Switzerland) connected for transferring the solutions from tanks into the unit. Afterwards, the solutions proceed to a filtration stage with cut-off size of 5 μm (cartridge filters, ATLAS FILTRI, Italy), which ensures that minimum solid traces can pass to the membrane. Additionally, the plant involves a control panel for all the electrical connections of flowmeters and sensors (Omega, UK) positioned for the on-line monitoring of flow, pressure and temperature at the inlet and outlet streams. The stream salinity was surveilled by installed digital conductivity meters (Model Orion VersaStar Pro, by Thermo Fisher Scientific, US). The pilot-plant allows automatic operation using LabVIEW software (National Instrument, US) where the operational safety is considered by setting alarms to detect any potential hazard.

3. Experimental Procedure

The experimental testing encompasses evaluating the OC pilot plant for achieving different feed recovery rates under different operating conditions by conducting several trials using the TFC HF membrane. First, the intrinsic properties of the membranes were investigated at different temperature in the range of 20-30 °C. Thereafter, various experiments were accomplished for achieving four feed recovery percentages of 60%, 68%, 75% and 90% where the DS dilution was maintained at 75%. Each experiment was performed at a surrounding temperature of 27 °C and for 4 hours. The role of DS flowrate on OC performance was examined at constant FS flowrate of 1.10 L·min^{-1} by testing three DS flowrates of 0.28, 0.35 and 0.45 L·min^{-1} at 27 °C for 2 hours. Lastly, the long-term stability of the OC pilot-plant was evaluated for 48 hours at the 75% feed recovery as an intermediate condition with low risk of membrane stress. However, the experiment was performed at a surrounding temperature of 17 °C, which enabled the assessment of temperature influence on the OC performance.

All sets of conducted experiments were duplicated to check how successful the system is in giving reproducible data. Therefore, experimental outcomes were reproducible with less than 5% error.

3-1. Membranes Intrinsic Properties

The water permeability coefficient A was found using deionized water feed using the TFC HF membrane. A pressure of 2 bar was applied to the module and the permeate was then collected for 60 seconds.

$$A = \frac{\text{Weight of permeate (kg)}}{\text{Membrane area (m}^2\text{)} \times \text{Pressure (bar)} \times \text{time (hour)}} \quad (1)$$

The value of salt permeability coefficient B was calculated from the coefficient A, effective osmotic pressure and salt rejection (R_{NaCl}) correlations.

$$B = A\Delta\pi_{eff}\frac{1-R_{NaCl}}{R_{NaCl}} \quad (2)$$

The salt rejection (R_{NaCl}) was measured by using 500 mg·L^{-1} FS, pressurizing the system to 2 bar, collecting permeate and measuring conductivity.

$$R_{NaCl} = \left(1 - \frac{\text{Conductivity of permeate}}{\text{Conductivity of feed}}\right) \times 100 \quad (3)$$

3-2. Experimental Testing of HF Membranes

The TFC-HF membrane was positioned horizontally with countercurrent flow of FS and DS having an inside-out configuration, with FS and DS being directed to bore and shell sides, respectively, as shown in Fig. 7.

The experiments were performed with small feed tank of 20 L that was placed on a digital balance (Mettler Toledo, USA). This is because of the small area of TFC-HF where few millimeters of water will be permeated by the membrane and accurate determination of water permeation would not be feasible if feed was taken directly from 5,000 L tank.

Using TFC-HF membrane and for the same small area limitation, higher percentage of feed water recovery will not be achieved by the once-through flow of FS. Therefore, the FS was made in recirculation mode by placing the outlet concentrated FS stream in the same inlet FS tank and the DS flow was kept in once-through mode. FS recirculation helps in concentrating the initial feed water tank with experimental time and makes the membrane capable of achieving higher recovery rates. Therefore, various feed recovery percentages were achieved by the manipulation in the feed concentration rather than changing the flowrates, which were kept constant at 1.5 L·min^{-1} as recommended by the membrane manufacturer.

The impact of tested membrane on the OC process operation was analyzed based on the measured water flux, RSF and specific reverse solute flux.

The weight difference of feed tank was recorded by the data acquisition system (LabVIEW, National Instrument, US) and was transferred into water flux values (LMH) when TFC-HF membrane was used.

$$J_w = \frac{W_{initial\ feed} - W_{final\ feed}}{t \times A} \quad (4)$$

where, J_w: is the water flux (LMH) and is calculated from difference between weight of initial feed water and final weight of water in feed tank ($W_{initial\,feed} - W_{final\,feed}$) (L) over the membrane area A (m^2) and time of experiment t (hours).

The conductivity of solutions measured from the conductivity detectors was transferred into NaCl mass flowrate and performing an overall mass balance allows determining the RSF.

$$J_{s,\,TFC\text{-}HF} = \frac{(W_{initial\,feed}C_{initial\,feed} - W_{final\,feed}C_{final\,feed}) \times 60}{AMw_s} \quad (5)$$

where and $J_{s,\,TFC\text{-}HF}$ are RSF ($mmol \cdot h^{-1} \cdot m^{-2}$) for the membrane, $C_{initial\,feed}$ and $C_{final\,feed}$ are the initial and final concentration in feed tank, $W_{initial\,feed}$ and $W_{final\,feed}$ are the initial and final weight of feed tank, A is the membrane area (m^2) and MW_s is the solute molecular weight ($mg \cdot mmol^{-1}$).

The metric parameter (J_s/J_w) is the specific salt flux indicating the FO performance and the solutes loss per water pass across the membrane ($mmol \cdot L^{-1}$).

RESULTS AND DISCUSSION

1. Impact of Temperature on Membranes Intrinsic Properties

The influence of operating temperature on the water and salt permeability coefficients (A and B) of FO membranes was investigated. Fig. 8 discloses the operating temperature effect studied in the range o (20-30 °C on the improvement of membrane permeability. Despite the fact that the transport parameters A and B are not relying on some operating conditions represented by flowrates and DS concentration [49], the depicted trends showed enhancement of both permeability coefficients at elevated temperature. The observed temperature role on increasing the water and salt permeability was also demonstrated for TFC membranes of various HF and flat sheet configurations [43,49-52]. It is reported that the higher A and B permeability coefficients at increased temperature are referred to the altered solutions' thermodynamic properties, including diffusivity and viscosity [51,53]. Indeed, the high temperature of FS and DS supports permeation by reducing the viscosity and enhancing diffusion. Therefore, the increased water and salt permeation are a consequence to the reduced viscosity of FS and DS that increases the diffusivity of water and salt molecules across the membrane surface. Fig. 8 shows that TFC-HF membrane testing under temperature from 19.70 to 30.50 °C, coefficient A and B was improved by 50.90% from 2.265 to 3.419 $LMH \cdot bar^{-1}$ and 48.90% from 0.319 to 0.475 LMH, respectively.

Results indicated that coefficients A and B values fitted a linear model with coefficient of determination above 0.99. Generally, the empirical correlations obtained between temperature and permeability coefficients are shown in Table 2.

Table 2. Empirical correlations of permeability coefficients using TFC-HF membrane

Membrane	A ($LMH \cdot bar^{-1}$)	B (LMH)
TFC-HF	$A_{TFC\text{-}HF}$=0.1075T+0.1185	$B_{TFC\text{-}HF}$=0.0146T+0.0265

2. Impact of Feed Recovery on the Feed Concentration

Different rates of feed recovery were obtained by the manipulation of feed concentration with time, hence changing the concentration gradient during the testing of TFC-HF membrane. Fig. 9 shows the increase in the feed conductivity and feed recovery with time, where longer runs of OC pilot-system allow recovering higher percentage of feed water rather than shorter periods at the same flowrate conditions. The initial measured conductivity of the 2,000 $mg \cdot L^{-1}$ FS was 4,000 $\mu S \cdot cm^{-1}$ and reached 19,460 $\mu S \cdot cm^{-1}$ at the maximum-targeted feed recovery of 90%. Fig. 9 also illustrates that the OC system was capable of reaching 60%, 68%, 75% and 90% feed recovery after 2.2, 2.5, 2.8 and 3.7 hours, respectively, at the same flowrate of 1.5 $L \cdot min^{-1}$.

3. Impact of Feed Recovery on the OC Process Performance

The performance of OC pilot-plant utilizing 2,000 $mg \cdot L^{-1}$ FS and 40,000 $mg \cdot L^{-1}$ DS while operating for 4 hours continuously was studied using the TFC-HF FO membrane modules. Fig. 10 demonstrates the trends of average water flux (J_w) and RSF (J_s) for obtaining each feed recovery percent starting from 0% recovery. The recorded water flux of OC system was 11.40 LMH at 60% recov-

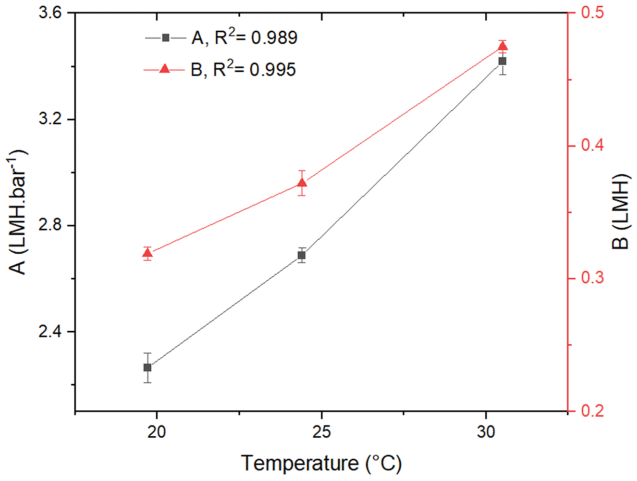

Fig. 8. Impact of temperature on the permeability coefficients of TFC-HF membrane.

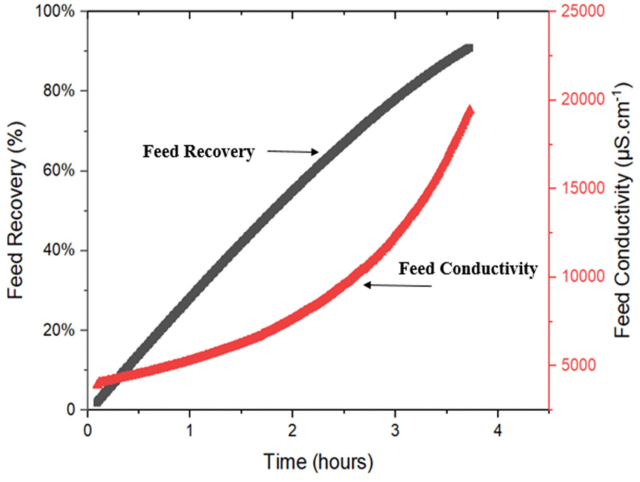

Fig. 9. Feed concentration (expressed as conductivity values) and feed recovery rate with time using TFC-HF membrane.

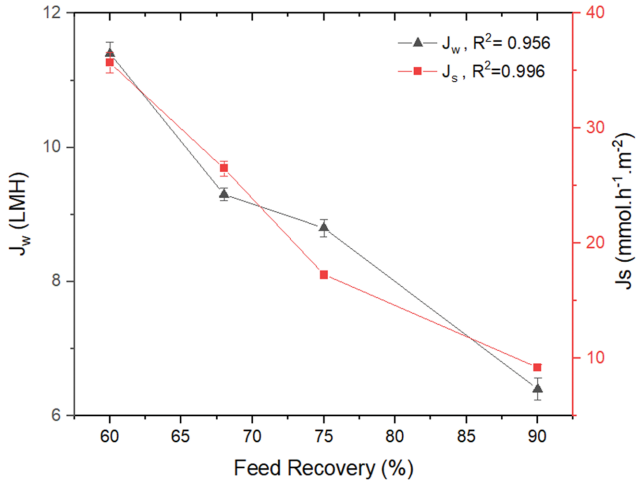

Fig. 10. Impact of changing the feed recovery percent on the water flux (J_w) and RSF (J_s).

ery and significantly dropping to 6.40 LMH at 90% recovery. Therefore, the experimental results confirmed the inverse proportion of flux with the recovery rate, which was demonstrated by the performance of several FO membranes in different systems [30,31,35]. During TFC-HF membrane testing, around 43.9% flux decline over 50% increase in feed recovery rate can be attributed to the diminished separation driving force as feed concentration increases with recovery percent. To further explain this, OC operation at high FS concentration level for achieving high recovery rate lowers the salinity difference between FS and DS across the membrane. Consequently, the descending water flux trend is assigned to the osmotic pressure difference reduction [12,35,54].

The rate of decline in the water flux of the studied TFC-HF membrane is lower than that we observed in our previous study for CTA-HF membrane [48]. Despite the fact that both membranes are of HF configuration, increasing the feed recovery rates from 60% to 90% corresponds to producing lower flux for CTA-HF than TFC-HF. The results emphasize the higher permeability of TFC-HF membrane acquired from the membrane material fabricated from aromatic polyamide chains. Xiao et al. [55] investigated CTA-based and TFC-based flat sheet membranes and proved the lower permeability of CTA rather than TFC. Several studies have tested the performance of the TFC membrane modules in FO process where the optimum water permeation obtained through trials with different DS and FS flowrates is reported as in Table 3.

RSF is another studied performance parameter for the operation of OC pilot-plant at the different feed recovery rates. Reverse solute diffusion refers to diffusion of the solute molecules (NaCl in this study) in the opposite direction to the anticipated conventional flow from FS to DS. Note that high RSF is translated into higher FS concentration and lower DS concentration, hence declining osmotic driving force and water flux [16]. Nevertheless, increased RSF phenomenon demands periodical replenishment to

Table 3. Water flux of several tested CTA and TFC HF membranes under different FS and DS flowrates

Membrane type	Membrane active area (m^2)	FS and DS used	Flowrates ($L \cdot min^{-1}$)	Highest water flux	Reference
CTA-HF	0.122	FS: DI* water, DS: 0.6 M NaCl solution	FS=0.05 DS=0.6	10 LMH	[56]
TFC-HF	2.3	FS: DI water and 35% NaCl solution, DS: 1 M NaCl solution	FS=2.33 DS=0.42	20.2 LMH for DI water as FS and 3.5 LMH for 35% NaCl solution as FS	[43]
			FS=1.67 DS=1.67	25.4 LMH for DI water as FS and 5.7 LMH for 35% NaCl solution as FS	
TFC-HF	0.0396	FS: DI water, DS: 5 M NaCl solution	FS flow giving Re#=600 DS flow giving Re=1,600	14 LMH	[37]
TFC-HF	0.0111	FS: DI water, DS: 1 M NaCl solution	Flow velocity of FS=0.74 m/s, DS=0.40 m/s	23.3 LMH	[57]
TFC-HF	0.5	FS: 2,000 $mg \cdot L^{-1}$ NaCl solution, DS: 40,000 $mg \cdot L^{-1}$ NaCl solution	FS=1.5 DS=1.5	11.4 LMH (at 60% feed recovery)	This work

DI*: deionized water, Re#: Reynolds Number.

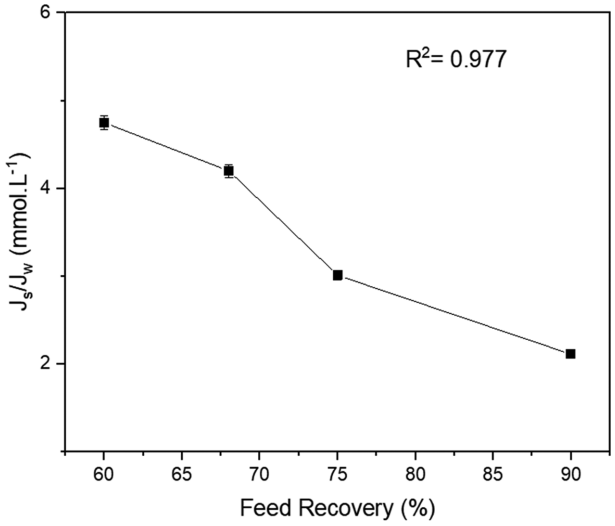

Fig. 11. Impact of changing the feed recovery percent on the specific solute flux (J_s/J_w) using TFC-HF membrane.

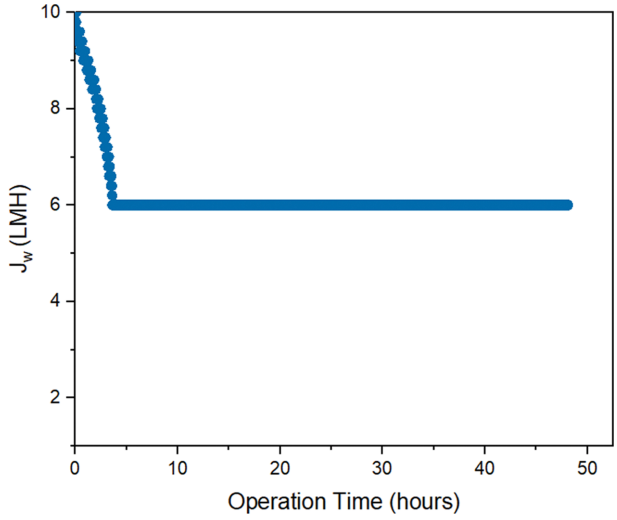

Fig. 12. Water flux trend with operating time during the long-term stability evaluation of OC process.

the DS concentration for recovering the separation driving force [58]. Fig. 10 shows a descending trend for the amount of solute transferred from DS into FS with the increase in the feed recovery rate. Apparently, the RSF was found high at low feed recovery percent similar to the water flux, hence RSF is directly proportional to the water flux behavior as reported in the study of Heo et al. [59]. The performance of OC pilot-plant using the TFC-HF membrane was recorded relatively low RSF values. For recovering 90% of feed, 9.20 mmol·h^{-1}·m^{-2} was the minimum flux of solutes reversing their flow from FS to DS. However, lowering feed recovery rate to 75%, 68% and 60% recorded higher calculated RSF values of 17.30, 26.50 and 35.70 mmol·h^{-1}·m^{-2}, respectively.

Fig. 11 illustrates that specific reverse solute flux, which estimates the loss in draw solutes per the water pass (J_s/J_w), exhibited a descending trend with feed recovery percent. Increasing the feed recovery rate from 60% to 90% reduced the loss of draw solutes per the water permeation from 3.12 to 1.43 mmol·L^{-1}. Note that a low value of (J_s/J_w) is preferable, since it indicates lower loss of the draw solution solutes [52,60].

4. Evaluating Long-term Stability of the OC Process

The OC process was operated for 48 hours at the experimental conditions required for achieving 75% feed recovery. This is because the operation at intermediate feed concentration can be described as being optimum since the achieved feed recovery percent (75%) and water flux (presented in section 3 of the results and discussion) are reasonably high enough with lower membrane exposure risk to fouling or increased stress.

Fig. 12 illustrates the water flux (J_w) trend for OC performance evaluation during the entire experimental time at 17 °C. The water flux trend demonstrated in Fig. 12 was achieved by changing the level of feed concentration to reach 75% feed recovery. At the beginning of the experiment, the obtained flux was 10.00 LMH. Following that with the increase in the feed recovery rate, the flux declined to 6.20 LMH after 3.60 hours when 75% of feed water was recovered. Subsequently, the flux maintained a steady trend at an average flux of 6.00 LMH throughout the remaining 44.4 hours of experimental time. In comparison with the experiment conducted at 27 °C for the same 75% feed recovery (section 3), the water flux at higher temperature was 46.70% higher (8.80 cf. 6.00 LMH), confirming the advantageous role of temperature in improving the water permeation across the membrane active layer.

5. Impact of DS Flowrate on the Membrane Performance

The performance of the OC process at each adjusted DS flowrate was studied by observing the trends of feed recovery, water flux, RSF and specific solute flux. It is obvious that higher DS flowrate has beneficial impact on increasing the feed recovery rate (Fig. 13). This explains that elevated DS flowrate facilitates higher permeation of feed water through the membrane. This high permeation rate can be a result of the evolved hydraulic pressure in the direction of DS [35]. Results in Fig. 13 indicate that the PA-TFC membrane enabled the OC process to reclaim from 37.30% up to 40.10% of feed when DS flowrate ranged from 0.28-0.45 L·min^{-1}.

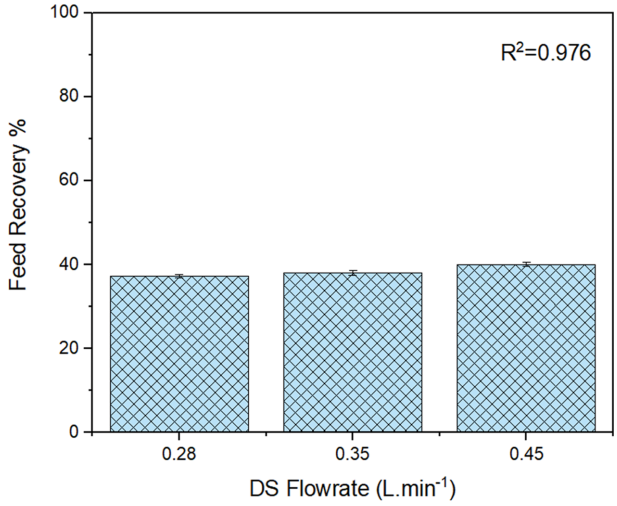

Fig. 13. Impact of changing DS flowrate on the feed recovery percent using TFC-HF membrane.

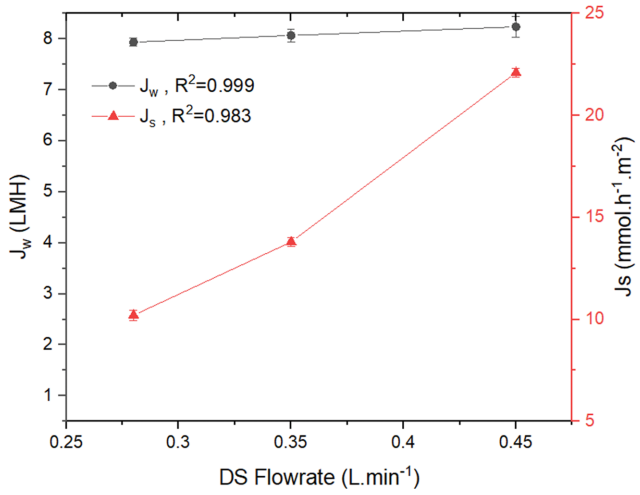

Fig. 14. Impact of changing DS flowrate on the water flux (J_w) and RSF (J_s) using TFC-HF membrane.

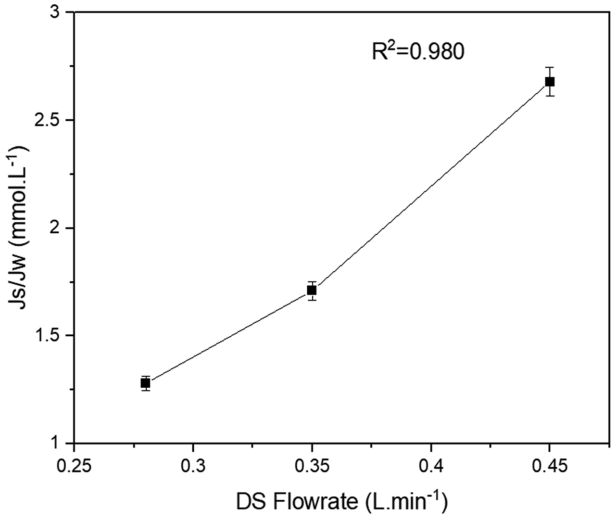

Fig. 15. Impact of changing DS flowrate on the specific solute flux (J_s/J_w) using TFC-HF membrane.

Fig. 14 shows the increasing trend of water flux (J_w) and RSF (J_s) with the DS flowrate. The average water flux values obtained for the membrane were 7.94, 8.07 and 8.24 LMH at DS flowrates of 0.28, 0.35 and 0.45 L·min^{-1}, respectively. This is translated into 3.78% flux enhancement for 60.71% increase in the DS flowrate. The water flux trend with DS flowrate was elucidated through previous research study based on average concentration inside TFC-HF module utilized in pilot-scale FO process [43]. This study explained that high DS flowrate, hence low residence time, increases the average concentration of draw solutes in the module. It is commonly recognized that maximum concentration to be reached in the membrane module is the initial concentration of DS. This initial DS concentration is approached asymptotically at higher DS flowrate. Subsequently, the high water flux at elevated DS flowrate is assigned to the considerable net driving force created. The same study of Sanahuja-Embuena [43] reported the influence of DS flowrate increase from 0.42 to 1.67 L·min^{-1}, improving the water flux from 19 to 25.4 LMH.

Similarly, the illustrated trends in Fig. 14 confirm that the natural phenomenon of solute back diffusion to the feed side was boosted at higher DS flowrate. DS flowrate adjusted from 0.28 to 0.45 L·min^{-1} prompted high occurrence of reverse solutes diffusion that was increased from 10.20 to 22.10 mmol·h^{-1}·m^{-2} across the membrane TFC in the examined DS flowrate range. Of note is that lower RSF obtained at lowest studied DS flowrate is desirable since it produces minimal reduction in the driving force and excludes the need for DS re-concentration. The straightforward relation of RSF with the water flux is also confirmed in these experiments.

Fig. 15 displays the impact of DS flowrate on the specific reverse solute flux (J_s/J_w). It is obvious that increasing the DS flowrate results in increasing the draw solute loss per water pass. The draw solute loss was boosted from 1.29 to 2.68 mmol·L^{-1} when DS flowrate was elevated from 0.28 to 0.45 L·min^{-1}.

CONCLUSIONS

This study investigated the performance of PA-TFC HF membrane for feed concentration at pilot-scale level. The implemented OC process targets the concentration of synthetic prepared FS mimicking the real PW salinity from Qatari's gas industries using DS of salinity representative to the local seawater. The OC pilot-plant performance was evaluated for achieving different feed recovery rates and operating under different flow rates and temperatures. Examining the obtained trends of water flux, RSF and specific reverse solute flux reveal:

a. High feed recovery percent was achieved by concentrating the FS according to the recirculation mode of operation of the membrane. The obtained results revealed that the highest feed recovery of 90% at constant DS dilution of 75% was successfully achieved at FS conductivity increase from 4,000 µS·cm^{-1} to 19,460 µS·cm^{-1}.
b. An increase in the rate of feed water recovery slightly lowered the produced water flux. The water flux of the OC process at 27 °C was found to be decreasing from 11.40 to 6.40 LMH.
c. Operation at high feed recovery percent is translated into lower RSF and specific reverse solute trends and is preferable to lower the back diffusivity of solutes from DS to FS, hence the osmotic pressure gradient across the membrane is maintained.
d. The long-term stability of OC pilot-plant was validated for a continuous 48 hour run at the optimum conditions for recovering 75% of feed and at 17 °C. The membrane succeeded in recovering the feed at an average water flux of 6.00 LMH, with minimal flux decline throughout the long-term run.
e. High DS flowrate had a beneficial impact on increasing the feed recovery rate and water permeation through the membrane; however, it had an adverse role in increasing the RSF. At DS flowrate of 0.45 L·min^{-1}, a maximum water flux of 8.24 LMH was achieved by which recovering 40.10% of the feed.
f. Water and salt permeability coefficients of the membrane were improved at a higher temperature, owing to the reduced viscosity and enhanced diffusion of FS and DS. Results showed that the TFC-HF module has A and B values of 3.419 LMH·bar^{-1} and 0.475 LMH, respectively, at the highest tested temperature

of 30 °C.

ACKNOWLEDGEMENT

This work was made possible by the support of a National Priorities Research Program (NPRP) grant from the Qatar National Research Fund (QNRF), grant reference number NPRP10-0118170191. The statements made herein are solely the responsibility of the authors. The authors would like to thank Dan Jerry Cortes from Qatar University and Arnold Janson from ConocoPhillips, Qatar for providing useful information for this paper.

REFERENCES

1. M. I. H. Ansari, A. Qurashi and M. K. Nazeeruddin, *J. Photochem. Photobiol. C Photochem. Rev.*, **35**, 1 (2018).
2. S. Adham, A. Hussain, J. Minier-Matar, A. Janson and R. Sharma, *Desalination*, **440**, 2 (2018).
3. T. Y. Cath, A. E. Childress and M. Elimelech, *J. Memb. Sci.*, **281**, 70 (2006).
4. B. Van Der Bruggen and P. Luis, *Rev. Chem. Eng.*, **31**, 1 (2015).
5. T. S. Chung, L. Luo, C. F. Wan, Y. Cui and G. Amy, *Sep. Purif. Technol.*, **156**, 856 (2015).
6. I. L. Alsvik and M. B. Hägg, *Polymers (Basel)*, **5**, 303 (2013).
7. X. Bao, Q. Wu, J. Tian, W. Shi, W. Wang, Z. Zhang, R. Zhang, B. Zhang, Y. Guo, S. Shu and F. Cui, *Chem. Eng. J.*, **370**, 262 (2019).
8. W. C. L. Lay, T. H. Chong, C. Y. Tang, A. G. Fane, J. Zhang and Y. Liu, *Water Sci. Technol.*, **61**, 927 (2010).
9. K. Lutchmiah, A. R. D. Verliefde, K. Roest, L. C. Rietveld and E. R. Cornelissen, *Water Res.*, **58**, 179 (2014).
10. N. M. Mazlan, D. Peshev and A. G. Livingston, *Desalination*, **377** 138 (2016).
11. C. Klaysom, T. Y. Cath, T. Depuydt and I. F. J. Vankelecom, *Chem. Soc. Rev.*, **42**, 6959 (2013).
12. V. Yangali-Quintanilla, Z. Li, R. Valladares, Q. Li and G. Amy, *Desalination*, **280**, 160 (2011).
13. A. Haupt and A. Lerch, *Membranes (Basel)*, **8**, 47 (2018).
14. S. Zhao, L. Zou, C. Y. Tang and D. Mulcahy, *J. Memb. Sci.*, **396**, 1 (2012).
15. M. Perry, https://www.forwardosmosistech.com/how-forward-osmosis-performance-is-limited-by-concentration-polarization, Accessed 20 August 2019 (2013).
16. S. Lee, C. Boo, M. Elimelech and S. Hong, *J. Memb. Sci.*, **365** 34 (2010).
17. C. Boo, M. Elimelech and S. Hong, *J. Memb. Sci.*, **444**, 148 (2013).
18. Q. Ge, M. Ling and T. S. Chung, *J. Memb. Sci.*, **442**, 225 (2013).
19. S. Munirasu, M. A. Haija and F. Banat, *Process Saf. Environ. Prot.*, **100**, 183 (2016).
20. L. Chekli, S. Phuntsho, J. E. Kim, J. Kim, J. Y. Choi, J. S. Choi, S. Kim, J. H. Kim, S. Hong, J. Sohn and H. K. Shon, *J. Memb. Sci.*, 497 (2016).
21. D. J. Johnson, W. A. Suwaileh, A. W. Mohammed and N. Hilal, *Desalination*, **434**, 100 (2018).
22. J. E. Kim, J. Kuntz, A. Jang, I. S. Kim, J. Y. Choi, S. Phuntsho and H. K. Shon, *Process Saf. Environ. Prot.*, **127**, 180 (2019).
23. R. Jalab, A. M. Awad, M. S. Nasser, J. Minier-Matar, S. Adham and S. J. Judd, *Water Res.*, **163**, 114879 (2019).
24. J. Veil and C. Clark, *SPE Prod. Oper.*, **26**, 234 (2011).
25. J. Veil, U.S Produced Water Volumes and Management Practices in 2012 (2015).
26. K. L. Hickenbottom, N. T. Hancock, N. R. Hutchings, E. W. Appleton, E. G. Beaudry, P. Xu and T. Y. Cath, *Desalination*, **312**, 60 (2013).
27. J. Minier-Matar, A. Santos, A. Hussain, A. Janson, R. Wang, A. G. Fane and S. Adham, *Environ. Sci. Technol.*, **50**, 6044 (2016).
28. J. Minier-Matar, A. Hussain, A. Janson, R. Wang, A. G. Fane and S. Adham, *Desalination*, **376**, 1 (2015).
29. S. Phuntsho, S. Sahebi, T. Majeed, F. Lotfi, J. E. Kim and H. K. Shon, *Chem. Eng. J.*, **231**, 484 (2013).
30. A. H. Hawari, N. Kamal and A. Altaee, *Desalination*, **398**, 98 (2016).
31. S. J. Im, G. W. Go, S. H. Lee, G. H. Park and A. Jang, *Desalin. Water Treat.*, **57**, 24583 (2016).
32. S. Phuntsho, S. Vigneswaran, J. Kandasamy, S. Hong, S. Lee and H. K. Shon, *J. Memb. Sci.*, **415-416**, 734 (2012).
33. S. Chakrabortty, M. Pal, M. Roy and P. Pal, *Desalination*, **365**, 329 (2015).
34. S. J. Im, S. Jeong and A. Jang, *J. Memb. Sci.*, **549**, 366 (2018).
35. M. S. Thabit, A. H. Hawari, M. H. Ammar, S. Zaidi, G. Zaragoza and A. Altaee, *Desalination*, **461**, 22 (2019).
36. J. Ren and J. R. McCutcheon, *Desalination*, **343**, 187 (2014).
37. T. Majeed, S. Phuntsho, S. Sahebi, J. E. Kim, J. K. Yoon, K. Kim and H. K. Shon, *Desalin. Water Treat.*, **54**, 817 (2015).
38. J. T. Arena, S. S. Manickam, K. K. Reimund, P. Brodskiy and J. R. McCutcheon, *Ind. Eng. Chem. Res.*, **54**, 11393 (2015).
39. W. Suwaileh, N. Pathak, H. Shon and N. Hilal, *Desalination*, **485**, 114455 (2020).
40. S. Mansouri, S. Khalili, M. Peyravi, M. Jahanshahi, R. R. Darabi, F. Ardeshiri and A. S. Rad, *Korean J. Chem. Eng.*, **35**, 2256 (2018).
41. B. Bolto, J. Zhang, X. Wu and Z. Xie, *Membranes (Basel)*, **10**, 4 (2020).
42. Oasys Water, http://oasyswater.com/solutions/technology/ (Accessed 27 April 2020).
43. V. Sanahuja-Embuena, G. Khensir, M. Yusuf, M. F. Andersen, X. T. Nguyen, K. Trzaskus, M. Pinelo and C. Helix-Nielsen, *Membranes (Basel)*, **9**, 66 (2019).
44. R. Wang, L. Shi, C. Y. Tang, S. Chou, C. Qiu and A. G. Fane, *J. Memb. Sci.*, **355**, 158 (2010).
45. T. Majeed, F. Lotfi, S. Phuntsho, J. K. Yoon, K. Kim and H. K. Shon, *Desalin. Water Treat.*, **53**, 1744 (2015).
46. W. Wang, Y. Guo, M. Liu, X. Song and J. Duan, *Korean J. Chem. Eng.*, **37**, 1573 (2020).
47. S. M. Mirkhalili, S. A. Mousavi, A. R. Saadat Abadi and M. Sadeghi, *Korean J. Chem. Eng.*, **34**, 3170 (2017).
48. R. Jalab, A. M. Awad, M. S. Nasser, J. Minier-matar and S. Adham, *J. Environ. Chem. Eng.*, **8**, 104494 (2020).
49. Q. Wang, Z. Zhou, J. Li, Q. Tang and Y. Hu, *Desalination*, **452**, 75 (2019).
50. L. Feng, L. Xie, G. Suo, X. Shao and T. Dong, *Trans. Tianjin Univ.*, **24**, 571 (2018).
51. M. R. Chowdhury and J. R. McCutcheon, *J. Memb. Sci.*, **553**, 189 (2018).

52. J. Ren, M. R. Chowdhury, J. Qi, L. Xia, B. D. Huey and J. R. McCutcheon, *J. Memb. Sci.*, **540**, 344 (2017).
53. S. J. You, X. H. Wang, M. Zhong, Y. J. Zhong, C. Yu and N. Q. Ren, *Chem. Eng. J.*, **198-199**, 52 (2012).
54. R. A. Maltos, J. Regnery, N. Almaraz, S. Fox, M. Schutter, T. J. Cath, M. Veres, B. D. Coday and T. Y. Cath, *Desalination*, **440**, 99 (2018).
55. T. Xiao, L. D. Nghiem, J. Song, R. Bao, X. Li and T. He, *Sep. Purif. Technol.*, **186**, 45 (2017).
56. M. Shibuya, M. Yasukawa, T. Takahashi, T. Miyoshi, M. Higa and H. Matsuyama, *Desalination*, **362**, 34 (2015).
57. S. Zhao, J. Minier-Matar, S. Chou, R. Wang, A. G. Fane and S. Adham, *Desalination*, **402**, 143 (2017).
58. N. Akther, A. Sodiq, A. Giwa, S. Daer, H. A. Arafat and S. W. Hasan, *Chem. Eng. J.*, **281**, 502 (2015).
59. J. Heo, K. H. Chu, N. Her, J. Im, Y. G. Park, J. Cho, S. Sarp, A. Jang, M. Jang and Y. Yoon, *Desalination*, **389**, 162 (2016).
60. D. L. Shaffer, J. R. Werber, H. Jaramillo, S. Lin and M. Elimelech, *Desalination*, **356**, 271 (2015).